CrossMark

ORIGINAL PAPER

Modeling forest fires in Mazandaran Province, Iran

Amir T. Payandeh Najafabadi[1] · Fatemeh Gorgani[2] · Maryam Omidi Najafabadi[3]

Abstract We used a spatio-temporal shot-noise Cox process to study the distribution of forest fires reported between 2006 and 2010 in the Mazandaran Province's forests. The fitted model shows that daily temperature, altitude, and slope-exposure impacted fire occurrence. Forest fire occurred in the region had an aggregated behavior, which increased in radius below 1-km away from fired areas; a periodic pattern of fire occurrence in the region was verified. The risk of forest fire is significantly higher for areas with southern exposure and slope between 30° and 50°, northern exposure and slope between 0° and 50°, and eastern exposure and slope between 0° and 30°. The risk of fire was also significantly higher at altitudes between 1350 and 3000 m asl. Human causes were the main ignition source for forest fires in the region. The fire occurrence rate stayed above average during the drought period from September 2008 to September 2009. Our findings could lead to the development of fire-response and fire-suppression strategies appropriate to specific regions.

✉ Amir T. Payandeh Najafabadi
amirtpayandeh@sbu.ac.ir

[1] Faculty Member of Department of Mathematical Sciences, Shahid Beheshti University, G.C. Evin, Tehran 1983963113, Iran

[2] Department of Basic Sciences, Payame Noor University Centre, Tehran, Iran

[3] Faculty Member of Department of Agricultural Sciences, Science and Research Branch, Islamic Azad University, Tehran, Iran

Introduction

Most of Iran is covered in desert and it ranks as the 56th lowest jungle country in the world. Iranian land cover from forests is less than 0.25 ha ind^{-1}, considerably less than international standard 0.8 ha ind^{-1} (Khosroshahi and Ghavami 2005). Northern Iran borders the southern shore of the Caspian Sea, and the regional climate supports a considerable amount of temperate and dense forest (2.1 million ha out of 14.2 million ha across the country) with broad leaf trees from the third geological age, which play a vital role in Iranian ecosystems. Mazandaran Province is located beside the Caspian Sea (Fig. 1). The forests of Mazandaran extend to about 1.5 million ha and are the most significant forests in northern Iran.

Mazandaran forests are mostly located at high altitude (more than 2500 m asl. in some parts) and as such are low touched forests. Unfortunately, hundreds of hectares of these forests are burned every year [about 300–400 ha (BanjShafieia et al. 2010; HassanNayebi 2003)]. Many researchers indicate that human activity is the main cause of fire ignition in the area. The U. N. Food and Agriculture Organization's (FAO) reports in 2002 and 2010 stated that approximately 0.06 % of Iran's forest burns every year.

Forest fires are an extremely complex phenomenon and occur naturally from events such as lightning strike, but there are other causes such as human negligence, accidents and intentional human activity; for example, arson (illegal fires started deliberately with malicious intent). Research into forest fires has been done for many countries including Iran. Such research has mostly focused on modeling forest

🖄 Springer

Fig. 1 Mazandaran Province inside Iranian map

fires to minimize the impact of expected and unexpected fires on forests. The spatial pattern of fire occurrence is a major focus of studies on the dynamics of forest fires and their role in determining landscape structure and composition of vegetation species within a forest environment (Turner and Romme 1994; Guyette et al. 2002; Ryan 2002; Larjavaara et al. 2005; Mermoz et al. 2005). There are many inherent stochastic factors that contribute to fire occurrence; therefore researchers have applied stochastic models. Moreover, several searches in the U.S. have shown that fires caused by arson (which accounted for up to 80 % of all fires reported in the U.S.) cluster in dimensions of time (Prestemon and Butry 2005), space and space–time (Gralewicz et al. 2011). This has contributed to the increasing popularity of spatio-temporal point process models as an alternative to more computationally demanding deterministic models.

Studies evaluating histories of fire occurrences began early in the twentieth century, mostly in the U.S. and Canada. These early studies analyzed the extent of fire occurrences (for an excellent review see McKenzie et al. 2000). A large number of studies on forest fires apply a static analysis rather than attempting a dynamic approach that takes into account the stochastic spatial distribution of forest fires. Some of most influential dynamic attempts to study forest fires include statistical modeling of forest fires initiated by Dayananda (1977), which introduced stochastic modeling of the pattern of fire occurrence in a given forest. Pew and Larsen (2001) analyzed spatial and temporal patterns of human-caused fires using a GIS dataset. Martínez and Chuvieco (2003) employed a spatial distribution pattern model to classify Spanish municipalities according to their actions regarding properties of forest fire. Peng et al. (2005) used a temporal model to estimate conditional

occurrence of natural fires in a Los Angeles forest. Brillinger et al. (2006) evaluated the probability of fires occurring in some specific points in a Californian forest. Yang and He (2007) analyzed human-caused fires in a spatial pattern using the Poisson process model. Amatulli et al. (2007) reported that fires caused by human activity in the Arago'n forest were more spatially diffuse than those caused by lightning. Benavent-Corai et al. (2007) demonstrated that human impact had important implications in terms of decreasing inter-event intervals and increasing the sparking frequency for forest fire modeling. Following the method introduced by Martínez and Chuvieco (2003), Chas-Amil et al. (2010) employed spatial analysis to characterize the distribution of causes and motivation for intentional fire lighting and wild fires in Galicia (northwestern Spain). Couce and Knorr (2010) employed a cellular automata (CA) model to adjust the spatial distribution of more than 750,000 African wild fires detected in 2003. Wang and Anderson (2010) used K-function and kernel estimation methods to determine that annual differences in spatial patterns of fires caused by humans tended to be more clustered with more complex spatial patterns than those caused by lightning. Moreover, the models demonstrated that human-caused fires in 2003–2007 were highly concentrated in southern Alberta, Canada, indicating the existence of an interaction between space and time. Gralewicz et al. (2011) presented a method to identify baseline expectations and ignition trends between 1980 and 2006 across 1-km spatial units. Jiang et al. (2012) determined that the traditional Poisson model overestimated fire occurrence during the fire season (May through August) in a Canadian forest.

Some interesting research has been done on forest fire spatial distribution and its impact on Iranian ecology. Azizi and Yousofi (2009) studied the ecological impact of forest fires reported between December 16–21, 2005 in forests in Gilan and Mazandaran Provinces. Mohammadi et al. (2010) used GIS information with the Analytical Hierarchy Process (AHP) method to evaluate the impact of vegetation, physiographic and weather factors, human activity and distance to rivers and roads on fires in a part of the Paveh forest. Ardakani et al. (2011) demonstrated that data generated by the Moderate Resolution Imaging Spectroradiometer (MODIS) were a valuable source of data used to investigate different phases of fire management in Iranian forests. Following the work of Mohammadi et al. (2010), Mahdavi et al. (2012) employed the AHP method to study a forest in Ilam Province.

We employed a spatio-temporal shot-noise Cox process introduced by Møller and Diaz-Avalos (2010) to: (i) identify influential and significant factors and covariates that impact on Mazandaran forest fires; (ii) determine spatial and temporal structures of fire occurrence in Mazandaran

forests; and (iii) explain spatial and temporal variation in occurrences of these fires.

In "Materials and methods" section reviews some concepts of spatial point process modeling, including shot-noise Cox processes, which play a crucial role in the rest of this article. In "Results" section gives results from application of a spatio-temporal shot-noise Cox process to fires reported in 2005–2011 in Mazandaran forests, and in "Conclusion and discussion" section presents a discussion and conclusions based on these findings.

Materials and methods

Spatio-temporal shot-noise Cox-processes

Spatial point processes are a form of mathematical model, which take into account GIS information to identify observed spatial pattern in terms of them being random, regular, or cluster patterns of specific objects in a plane or in a space. Spatio-temporal point processes are an extension of spatial point processes that take into account time as well as space in their models and are termed time–space processes. Standard practice in analysis of spatio-temporal point processes is the employment of a first step to form an estimate of the average function $\lambda(u, t)$ for $u \in R^2$ (u, t), $t \in Z$. This average function can then be employed to study several properties of the spatio-temporal point process. Then, if the estimated average function is deemed to be uniform, $\lambda(\boldsymbol{u}, t) \equiv \lambda$, it is used to investigate inter-point interactions by estimating various summary statistics such as the F-function (distribution function for distance between a given point and the nearest event; for example, empty space) and the L-function (distribution function for distance between a given event and a nearest event, say, nearest-neighbor). These statistics are compared with their expected values for the homogeneous Poisson point process that serves as the null hypothesis of complete spatial randomness (CSR); that is, absence of an interaction (Ripley 1976; Diggle 1983). Therefore, testing the CSR hypothesis is an important part of exploratory data analysis in a spatial point process. If the CSR hypothesis is rejected, then one proceeds to investigate the spatial correlations in a given pattern and period of time.

We used the Spatstat package (Baddeley and Turner 2005) available in the R statistical software system for analysis. A spatio-temporal shot-noise Cox process is a spatial point process which can be viewed as a doubly stochastic Poisson process. The time dependent average function of a spatio-temporal shot-noise Cox process can be restated as:

$$\lambda(\boldsymbol{u}, t) = \lambda_1(\boldsymbol{u})\lambda_2(t)S(\boldsymbol{u}, t) = \lambda_1(\boldsymbol{u})\lambda_2(t)$$
$$= \sum_{i=-\infty}^{\infty} \sum_{\boldsymbol{q} \in \Phi_{\boldsymbol{u}}} \frac{\psi(\boldsymbol{u} - \boldsymbol{q}, t - i)}{\omega} \quad (1)$$

where, $\lambda_1(\boldsymbol{u})$ and $\lambda_2(t)$ are non-negative deterministic functions (which usually are determined by regression methods, see below), $S(\boldsymbol{u}, t)$ is a spatio-temporal process with unit mean (i.e., $E(S(\boldsymbol{u}, t)) = 1$), Φ_u is a stationary Poisson process with intensity $\omega > 0$ and $\psi(\cdot, \cdot)$ is a joint density on $\Re^2 \times Z$ with respect to the product measure of Lebesgue measure on $\Re^2$ and counting measure on Z. The kernel $\psi(\cdot, \cdot)$ is separable whenever $\psi(\boldsymbol{u}, t) = \phi(\boldsymbol{u})\chi(t)$ for all $(\boldsymbol{u}, t) \in \Re^2 \times Z$ where $\phi(\cdot)$ is a density function on $\Re^2$ and $\chi(t)$ is a probability density function on Z. See Møller and Waagepetersen (2007) for more details on the spatio-temporal shot-noise Cox processes.

Suppose that some related covariate information about temporal and spatial components of the observed pattern is given. Moreover, suppose that such covariate information can be restated into discrete random variables $V^{(1)}(\boldsymbol{u}), \ldots, V^{(p)}(\boldsymbol{u})$ for spatial information $\boldsymbol{u}$ and $T^{(1)}(t), \ldots, T_{(m)}(t)$ for temporal information t. Using such covariate variables, one may consider two following Poisson regression models for spatial intensity function $\lambda_1(\boldsymbol{u})$ and temporal intensity function $\lambda_2(t)$

$$ln(\lambda_1(\boldsymbol{u})) = \beta_0 + \sum_{j=1}^{p} \sum_{i=1}^{I_j} \beta_i^{(j)} I\left(V^{(j)}(\boldsymbol{u}) = i\right) + Error \quad (2)$$

$$ln(\lambda_2(t)) = \alpha_0 + \sum_{i=1}^{a} \alpha_i \cos(i\eta_t t) + \sum_{j=1}^{b} \alpha_j \sin(j\eta_t t)$$
$$+ \sum_{i=1}^{m} \gamma_i T^{(i)}(t) + Error \quad (3)$$

where, $I(\cdot)$ stands for the indicator function, $\{1,2,\ldots I_j\}$ represents support of discrete covariate $V^{(j)}(\boldsymbol{u})$, and $\eta_t = 2\pi/365$ for years with 365 days and $\eta_t = 2\pi/366$ for leap years. For identifiability of regression coefficients, one has to impose the bounds that $\Sigma_{i=1}^{I_j} \beta_i^{(j)} = 0$ for all $j = 1,2,\ldots p$. Regression coefficients β and α are estimated by least squares, while the constant coefficient m is determined by examining the Akaike information criterion (AIC).

For simplicity, this article assumes a separable kernel with form:

$$\psi(\boldsymbol{u}, t) = \phi(\boldsymbol{u}) \times \chi(t) = \frac{\exp\left\{-\frac{\|\boldsymbol{u}\|^2}{2\delta^2}\right\}}{2\pi\delta^2} \times \frac{2(t^* - t)}{t^*(t^* - 3)}, \quad (4)$$
$$t = 1, \ldots, t^* - 1$$

where, last significant lag t^* is determined by the auto-correlation function of the stochastic counting process N_t,

which represents the number of observed forest fires in an interval [0,t].

Inhomogeneous *K*- and *L*-functions

Møller and Waagepetersen (2004) introduced the following inhomogeneous *K*- and *L*-functions to investigate existence of random, regular, or cluster patterns for specific objects in a plane or space, under shot-noise Cox process X_t.

$$K(r,t) = 2\pi \int_0^r sg(s,t)ds, \quad L(r,t) = \sqrt{\frac{K(r,t)}{/pi}} \qquad (5)$$

where, $r = \|\boldsymbol{u}_1 - \boldsymbol{u}_2\|$ and $t = |t_1 - t_2|$ and $g(s,t)$ is the cross pair correlation function:

$$g((\boldsymbol{u}_1,t_1),(\boldsymbol{u}_2,t_2)) = 1 + \delta\psi \star \hat{\psi}(\boldsymbol{u}_1 - \boldsymbol{u}_2, t_1 - t_2) \qquad (6)$$

where $\star$ denotes convolution and $\hat{\psi}(\boldsymbol{u},t) = \psi(-\boldsymbol{u},-t)$.

Stoyan and Stoyan (2000) and Diggle et al. (2005) developed a 95 %-inter-quantile envelope for the $L(r) - r$ function based upon an MCMC simulation study. Using such a 95 %-inter-quantile envelope one may test the null hypothesis, H_0: the model fits the data, at the 0.05 confidence level. Whenever the observed $L(r) - r$ function falls into the 95 %-inter-quantile envelope obtained by simulating points under the fitted process X_t, one fails to reject the null hypothesis and concludes that the model fit is adequate.

Annual data for Mazandaran forest fires

This investigation used data on starting locations of 531 forest fires in Mazandaran forests reported from March 2006 to March 2010 (1826 days). The starting locations of these fires were used as spatio-temporal points. Calculations were based on the supposition that the stochastic counting process N_t stands for the number of daily forest fires reported in the region. Bessie and Johnson (1995), and Møller and Diaz-Avalos (2010) processed information on vegetation type, elevation, slope, exposure and temperature as covariate information that may impact on a forest fire in a given forest. Unfortunately, for this study information on vegetation type was not available from the relevant database. Therefore, this article considers altitude, $V^{(1)}(\boldsymbol{u})$, slope-exposure, $V^{(2)}(\boldsymbol{u})$, and average daily temperature (available at: http://www.mazandaranmet.ir/), of the region, $T(t)$, as covariate information that may affect a forest fire in the region. Altitude of the region averages approximately 1340 m asl. (Fig. 2a, b) and can be classified into 5 classes (Table 1).

Based on frequencies of slope and exposure, the area was classified into the 20 slope-exposure categories given in Table 2 and illustrated in Fig. 2c. The spatial pattern of

started forest fires from March 2006 to March 2010 in the area has been given by Fig. 2d.

Figure 3 represents average daily temperature, $T(t)$, of the region (Fig. 3a), the square root of the number of daily reported fires in the region, i.e., $\sqrt{N_t}$, for $t \in [0, 1826]$ (Fig. 3b), and autocorrelation of stochastic counting process N_t for different lags (Fig. 3c).

Using the above autocorrelation plot for different lags (Fig. 3, left panel), one cannot observe any significant autocorrelation after lag 32. Therefore, t^* in Model (3) can be taken equal to 32.

Results

Using the Spatstat package (Baddeley and Turner 2005, 2006) against starting location of such reported fire along with the above mentioned covariate variables $V^{(1)}(\boldsymbol{u})$, $V^{(2)}(\boldsymbol{u})$, and power of daily temperature $T(t)$, i.e., $T^{(i)}(t) \equiv T^{(i)}(t)$, for $i = 1,2,\ldots,m$. The spatial intensity function $\lambda_1(\boldsymbol{u})$ and temporal intensity function $\lambda_2(t)$ can be estimated as the following:

$$\ln\left(\hat{\lambda}_1(u)\right) = \sum_{i=1}^{5} \beta_i^{(1)} I\left(V^{(1)}(u) = E_i\right)$$
$$+ \sum_{i=1}^{20} \beta_i^{(2)} I\left(V^{(2)}(u) = SE_i\right) + Error \qquad (7)$$

$$\ln\left(\hat{\lambda}_2(t)\right) = -0.838\cos(\eta_t t) - 0.330\sin(\eta_t t)$$
$$+ 0.643\cos(2\eta_t t) - 0.719\sin(2\eta_t t)$$
$$+ \sum_{i=1}^{6} \gamma_i T^{(i)}(t) + Error \qquad (8)$$

where, $E_1,\ldots,E_5$ and $SE_1, SE_2,\ldots,SE_{20}$, respectively, represent values of discrete covariate $V^{(1)}$ and $V^{(2)}$, given above, and other estimated parameters are given by Table 3.

The maximum value for the exponent on daily temperature, $m = 6$, was found by taking the largest value of m that minimizes the AIC (AIC = 2581.697 for m = 6, while the AIC equaled 2615.269, 2586.638, and 2581.697 for m = 3, m = 4, and m = 5, respectively). Goodness of fit of the above spatio-temporal shot-noise Cox process model in spatial and spatio-temporal approaches was evaluated using a plot of the L(r) − r function and a 95 %-inter-quantile envelope obtained from 39 simulations from the fitted model. Figure 4 illustrates these plots.

Using regression parameters of estimated spatial average function λ_1 and temporal average function $\lambda_2(t)$ given by Eq. 2, one can conclude that: (1) risk of forest fire increased in areas with an altitude between 1350 m to 3000 m above sea level (corresponding to high positive
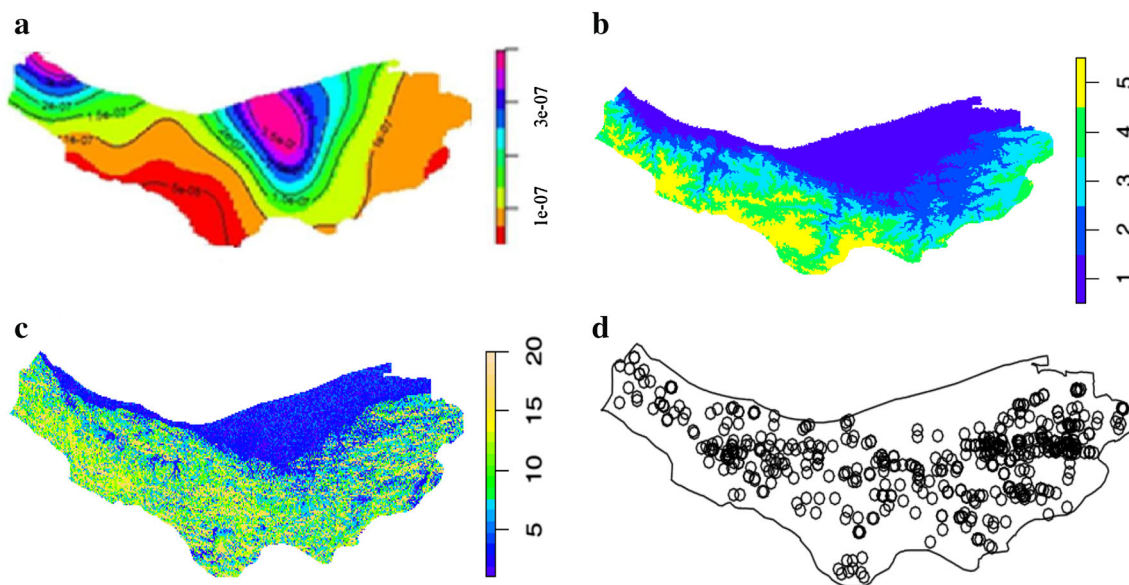
Fig. 2 **a** Topographic map of urban and rural regions in Mazandaran Province; **b** elevation map, in meters, above sea level in the area; **c** the 20 slope-exposure categories; **d** spatial pattern of started forest fire from March 2006 to 2010

Table 1 Altitude categories classification

Categories	Altitude above sea level (m)
E1	0–1350
E2	1350–2000
E3	2000–3000
E4	3000–4000
E5	4000–5000

Table 2 Slop-exposure categories classification

Topographical direction	Slop categories			
	0–15°	15°–30°	30°–50°	>50°
Flat	SE_4	SE_8	SE_{18}	SE_{20}
North	SE_3	SE_7	SE_{11}	SE_{13}
South	SE_5	SE_{17}	SE_{16}	SE_{19}
East	SE_1	SE_6	SE_9	SE_{12}
West	SE_2	SE_{10}	SE_{14}	SE_{15}

values of $\beta_3^{(1)}$ and $\beta_2^{(1)}$ and (2) the risk of forest fire in areas with a southern exposure and slope gradient of between 30° and 50°, northern exposure and slope gradient between 0° and 50°, northern exposure and slope gradient between 0° and 30° (corresponding to high positive values of $\beta_{16}^{(2)}, \beta_{19}^{(2)}, \beta_3^{(2)}, \beta_7^{(2)}, \beta_{11}^{(2)}, \beta_1^{(2)}$ and $\beta_6^{(2)}$ which are significantly higher than other areas.

Figure 4 shows that the $L(r) - r$ function for the spatial shot-noise Cox model is far away from the edges of its 95 % inter-quantile envelope (Fig. 4a). While the $L(r) - r$ function for the spatio-temporal shot-noise Cox model in most regions is close to the center line (red dash line) of its 95 % inter-quantile envelope (Fig. 4b). Therefore, one can conclude that the spatio-temporal shot-noise Cox model provides a more appropriate model compared to the spatial shot-noise Cox process. Moreover, Fig. 4 also demonstrates that the pattern of the spatio-temporal shot-noise Cox model for forest fires in the region is more aggregated than in an inhomogeneous Poisson process. Such aggregated spatial distribution dramatically increases in radiuses below 1 km away from the points for locations of fires (beginning part of solid line in Fig. 4b). This specific spatio-temporal and aggregate model verified the periodic spatial distribution of fire occurrence in the region and the fact that points close to fire areas have a higher chance of fire.

Figure 5 is a topographical map and realization graphs of the above estimated spatial average function $\lambda_1(u)$ and temporal average function $\lambda_2(u)$.

Comparing topographic maps of urban and rural regions in Mazandaran Province (Fig. 1) with the estimated spatial average function $\lambda_1(u)$ (Fig. 5a), it can be concluded that the risk of forest fire in the eastern half and southwest of the area (rural and tourist regions) are considerably higher than the risk in other areas. The rate of occurrence of forest fires in the period of study can be determined by the estimated temporal average function $\lambda_2(t)$ (Fig. 5b). Realization of the estimated temporal average function $\lambda_2(t)$ is given by Fig. 5c.
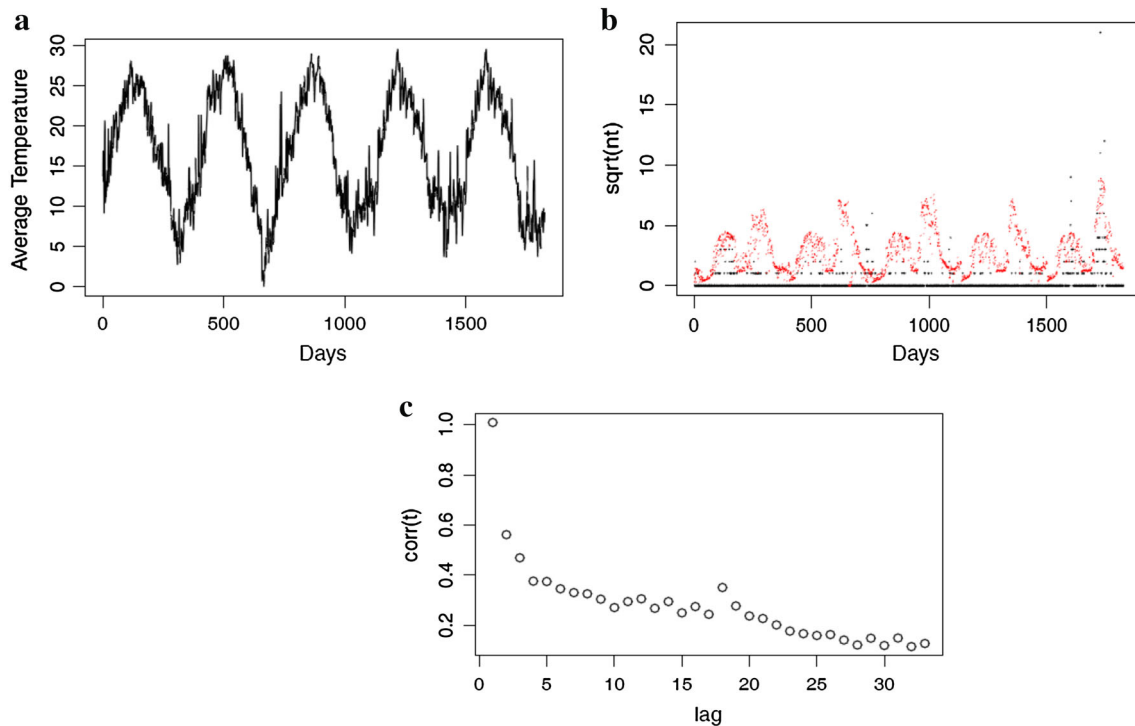
Fig. 3 a Average of daily temperature $T^{(1)}(t)$, for t ∈ [0, 1826]; **b** squared root of number of daily reported fire, i.e., $\sqrt{N_t}$, for ∈ [0, 1826]; and **c** autocorrelation stochastic counting process N_t for different lags

Table 3 Estimated parameters

| i	$\beta_i^{(1)}$	γ_i	$\beta_i^{(2)}$
1	−0.33748	−0.965570	0.48043
2	0.730622	−0.313965	0.87760
3	0.74201	0.1824225	0.84845
4	−0.44034	−0.549500	0.32017
5	−0.64430	−0.480520	0.18730
6		0.122520	0.92247
7			0.65450
8			0.19523
9			0.23502
10			0.76201
11			0.92678
12			−0.19400
13			−0.24170
14			−0.26698
15			0.19775
16			1.13200
17			0.73175
18			0.28710
19			0.94681
20			0.00001

Conclusion and discussion

This article employed a spatio-temporal shot-noise Cox process to: (**i**) determine factors that may impact forest fires and (**ii**) to identify areas at higher risk of fire in the forests of Mazandaran Province.

Using the fitted model, one may conclude that: (1) daily temperature (with polynomial order 6), altitude and slope-exposure impacted occurrence of forest fires in the region; (2) forest fire occurrence had an aggregated spatial distribution, which means that points close to areas of fire had more chance of fire occurrence compared to other areas. Moreover, fire chance dramatically increased in radiuses below 1 km away from areas of fire; (3) the risk of forest fire in the east and southwest of the area (rural and tourist regions) was considerably higher than the risk in other areas. These two observations were also reported in other research by HassanNayebi (2003) and, in a different context by Majidi et al. (2011); (4) fire occurrence was considerably higher in southwest Mazandaran Province (where elevation was lower than average in the province, at 1340 m above sea level), similar findings were reported in Ardakani et al. (2011); (5) the rate of forest fire occurrence stayed above average during drought periods (September
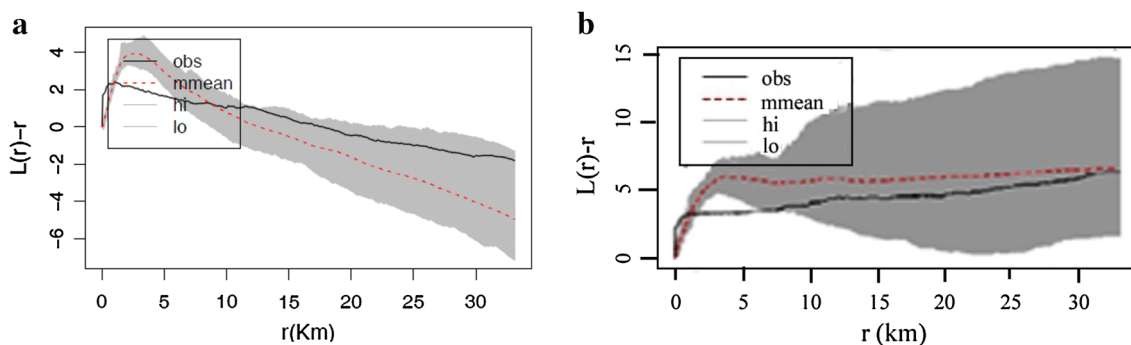
Fig. 4 Observed L(r) − r (*solid line* indicated by 'obs') along with their 95 % inter-quantile envelopes (*grey region* indicated by 'lo' and 'hi') obtained from 39 simulated observations from the fitted shot-noise-Cox model. Part **a** shows such L(r) − r from spatial model, while part **b** represents such estimations from spatio-temporal model
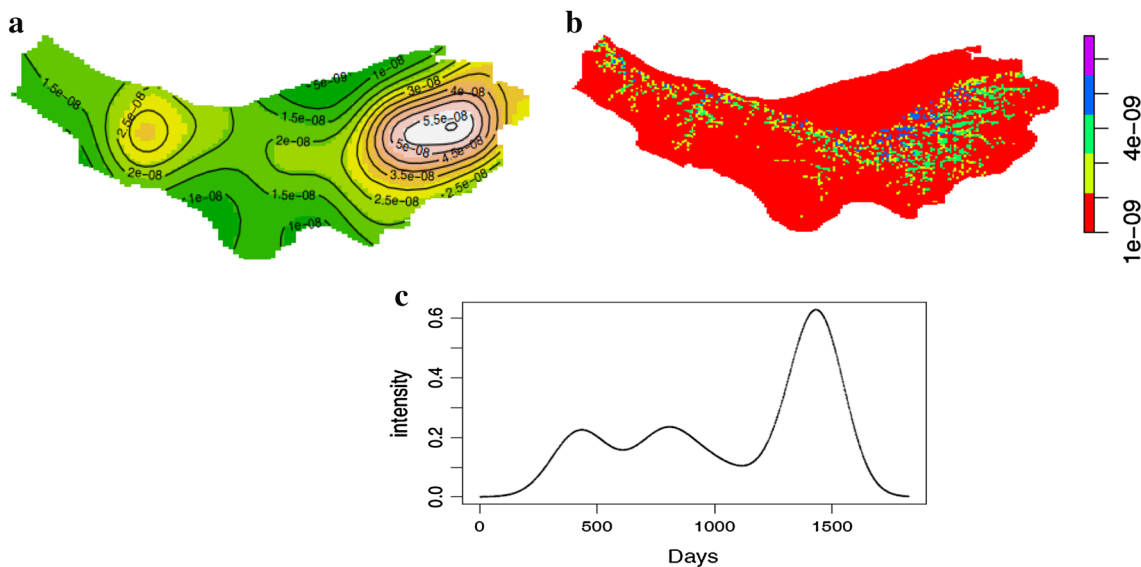
Fig. 5 a Topographic map of estimated spatial intensity function $\lambda_1(u)$; **b** realization of estimated spatial intensity function $\lambda_1(u)$; and **c** realization of estimated temporal intensity function $\lambda_2(u)$

2008 and September 2009, Tirandaz and Eslami 2012); (6) the periodic spatial distribution of fire occurrence in the region has also been reported by the U.N. FAO (2002, 2010); (7) risk of forest fire is significantly decreased in areas with an altitude higher than 3000 m above sea level.

The Model (7) provides useful spatial and temporal information that is not obvious or cannot be inferred from visual examination of raw data. Such quantitative knowledge could lead to the development of fire-response and fire-suppression strategies appropriate to specific regions within the province. The fitted model can be improved by using other general information on fires such as evaluations for area burned, date and time of ignition, weather conditions, causes and motivation, fire fighting measures and vegetation type as well as detailed information on the forest land affected (e.g., ownership, forest biomass of the area

and estimated losses). Unfortunately, such covariate information was not available in the Iranian forest fire database. More information would improve statistical forest fire models and consequently facilitate better fire management. Certainly, effective management practice requires an understanding of the role of biological and physical factors in patterns of fire occurrence in space and over time. Moreover, high quality information about space–time dynamics of fires can be developed by statistical models, which can be applied for long-term resource management of forest ecosystems and human property (McKenzie et al. 2000).

References

Amatulli G, Peréz-Cabello F, de la Riva J (2007) Mapping lightning/human-caused wildfires occurrence under ignition point location uncertainty. Ecol Model 200:321–333

Ardakani AS, Zoej MJV, Mohammadzadeh A, Mansourian A (2011) Spatial and temporal analysis of fires detected by MODIS data in Northern Iran from 2001 to 2008. Proc IEEE Geosci Remote Sens Soc Conf 4:216–225

Azizi A, Yousofi A (2009) Foehan and forest fire in Mazandaran and Gilan provinces: a Case study for the forest fire from December 16–21, 2005. Geogr Res 24:2–228

Baddeley A, Turner A (2005) An R package for analyzing spatial point patterns. J Stat Softw 12:1–42

Baddeley A, Turner R (2006) Modelling spatial point patterns in R. Case studies in spatial point pattern modelling. Lect Notes Stat 185:23–74

BanjShafieia A, Akbariniab M, Jalalib G, Hosseini M (2010) Forest fire effects in beech dominated mountain forest of Iran. For Ecol Manag 259:2191–2219

Benavent-Corai J, Rojo C, Suárez-Torres J, Velasco-García L (2007) Scaling properties in forest fire sequences: the human role in the order of nature. Ecol Model 205:336–342

Bessie WC, Johnson EA (1995) The relative importance of fuels and weather on fire behavior in subalpine forest. Ecology 76:747–762

Brillinger DR, Preisler HK, Benoit JW (2006) Probabilistic risk assessment for wildfires. Environmetrics 17:623–633

Chas-Amil ML, Touza J, Prestemon P (2010) Spatial distribution of human-caused forest fires in Galicia (NW Spain). In: Proceeding of the second international conference on modelling, monitoring and management of forest fires, pp 247–259

Couce E, Knorr W (2010) Statistical parameter estimation for a cellular automata wildfire model based on satellite observations. In: Proceeding of the second international conference on modelling, monitoring and management of forest fires, pp 37–47

Dayananda PWA (1977) Stochastic models for forest fires. Ecol Model 3:309–313

Diggle PJ (1983) Statistical analysis of spatial point patterns. Academic Press, London

Diggle PJ, Rowlingson B, Su T (2005) Point process methodology for on-line spatiotemporal disease surveillance. Environmetrics 16:423–434

Food and Agriculture Organization (FAO) (2002) General status of the food and agriculture statistics in Iran. Available at: www.faorap-apcas.org/docs/05Iran/No.2IRA.pdf

Food and Agriculture Organization (FAO) (2010) Global forest resources assessment 2010. Available at: www.fao.org/docrep/013/i1757e/i1757e.pdf

Gralewicz NJ, Nelson TA, Wulder MA (2011) Spatial and temporal patterns of wildfire ignitions in Canada from 1980 to 2006. Int J Wildland Fire 21:230–242

Guyette RP, Muzika RM, Dey DC (2002) Dynamics of an anthropogenic fire regime. Ecosystems 5:472–486

HassanNayebi Esmail (2003) Identifying and combating with different fires in forest. Extensional Programmes Institute, Tehran

Jiang Y, Zhuang Q, Mandallaz D (2012) Modeling large fire frequency and burned area in canadian terrestrial ecosystems with poisson models. Environ Model Assess 3:1–12

Khosroshahi M, Ghavami S (2005) Hoshdar book. Publications of Forest and Rangelands, Tehran

Larjavaara M, Kuuluvainen T, Rita H (2005) Spatial distribution of lightning-ignited forest fires in Finland. For Ecol Manag 208:177–188

Mahdavi A, Fallah Shamsi SR, Nazari R (2012) Forests and rangelands' wildfire risk zoning using GIS and AHP techniques. Casp J Environ Sci 10:43–52

Majidi E, Sobhani K, Rezaei MR (2011) Deforestation of forests in Iran. J Appl Environ Biol Sci 1:184–186

Martínez J, Chuvieco E (2003) Tipologías de incidencia y causalidad de incendios forestales basadas en an'alisis multivariante. Ecología 17:47–63

McKenzie D, Peterson DL, Agee JK (2000) Fire frequency in the interior Columbia River basin: building regional models from fire history data. Ecol Appl 10:1497–1516

Mermoz M, Kitzberger T, Veblen TT (2005) Landscape influences on occurrence and spread of wildfires in Patagonian forests and shrub lands. Ecology 86:2705–2715

Mohammadi F, Shabanian N, Pourhashemi M, Fatehi P (2010) Risk zone mapping of forest fire using GIS and AHP in a part of Paveh forests. Iran J For Poplar Res 18:586–595

Møller J, Diaz-Avalos C (2010) Structured spatio-temporal shot-noise Cox point process models, with a view to modelling forest fires. Scand J Stat 37:2–25

Møller J, Waagepetersen RP (2004) Statistical inference and simulation for spatial point processes. Chapman and Hall/CRC, Boca Raton

Møller J, Waagepetersen RP (2007) Modern statistics for spatial point processes. Scand J Stat 34(4):643–684

Peng RD, Schoenberg FP, Woods J (2005) A space-time conditional intensity model for evaluating a wildfire hazard index. J Am Stat Assoc 100:26–35

Pew KL, Larsen CPS (2001) GIS analysis of spatial and temporal pattern of human caused wildfire in the temperate rain forest of Vancouver island Canada. For Ecol Manag 140(1):1–8

Prestemon JP, Butry DT (2005) Time to burn: modeling wildland arson as an autoregressive crime function. Am J Agric Econ 87:756–770

Ripley BD (1976) The second-order analysis of stationary point processes. J Appl Prob 13:255–266

Ryan KC (2002) Dynamic interactions between forest structure and fire behavior in boreal ecosystems. Silva Fennica 36:13–39

Stoyan D, Stoyan H (2000) Improving ratio estimators of second order point process characteristics. Scand J Stat 27:641–656

Tirandaz M, Eslami A (2012) Zoning droughts and wetness trends in north of Iran: a case study of Guilan province. Afr J Agric Res 7:2320–2327

Turner MG, Romme WH (1994) Landscape dynamics in crown fire ecosystems. Landsc Ecol 9:59–77

Wang Y, Anderson KR (2010) An evaluation of spatial and temporal patterns of lightning- and human-caused forest fires in Alberta, Canada, 1980–2007. Int J Wildland Fire 19:1059–1072

Yang J, He HS (2007) Spatial patterns of modern period human caused fires in Missouri Ozrak highlands. For Sci 53:1–15